JACS
JOURNAL OF THE AMERICAN CHEMICAL SOCIETY
Article
pubs.acs.org/JACS

A Significant but Constrained Geometry Pt→Al Interaction: Fixation of CO_2 and CS_2, Activation of H_2 and $PhCONH_2$

Marc Devillard,[†,‡,▽] Richard Declercq,[†,‡,▽] Emmanuel Nicolas,[§,▽] Andreas W. Ehlers,[§] Jana Backs,[∥] Nathalie Saffon-Merceron,[⊥] Ghenwa Bouhadir,*[,†,‡] J. Chris Slootweg,*[,§] Werner Uhl,*[,∥] and Didier Bourissou*[,†,‡]

[†]Université de Toulouse, UPS, LHFA, 118 route de Narbonne, 31062 Toulouse, France

[‡]CNRS, LHFA, UMR 5069, 31062 Toulouse, France

[§]Department of Chemistry and Pharmaceutical Sciences, VU University Amsterdam, De Boelelaan 1083, 1081 HV Amsterdam, The Netherlands

[∥]Institut für Anorganische und Analytische Chemie der Westfälischen, Wilhelms-Universität Münster, Corrensstrasse 30, 48149 Münster, Germany

[⊥]Université Paul Sabatier, Institut de Chimie de Toulouse (FR 2599), 118 route de Narbonne, 31062 Toulouse cedex 9, France

Supporting Information

ABSTRACT: Reaction of the geminal PAl ligand [$Mes_2PC(=CHPh)AltBu_2$] (**1**) with [$Pt(PPh_3)_2$(ethylene)] affords the T-shape Pt complex [(**1**)$Pt(PPh_3)$] (**2**). X-ray diffraction analysis and DFT calculations reveal the presence of a significant Pt→Al interaction in **2**, despite the strain associated with the four-membered cyclic structure. The Pt···Al distance is short [2.561(1) Å], the Al center is in a pyramidal environment [Σ(C−Al−C) = 346.6°], and the PCAl framework is strongly bent (98.3°). Release of the ring strain and formation of X→Al interactions (X = O, S, H) impart rich reactivity. Complex **2** reacts with CO_2 to give the T-shape adduct **3** stabilized by an O→Al interaction, which is a rare example of a CO_2 adduct of a group 10 metal and actually the first with η^1-CO_2 coordination. Reaction of **2** with CS_2 affords the crystalline complex **4**, in which the PPtP framework is bent, the CS_2 molecule is η^2-coordinated to Pt, and one S atom interacts with Al. The Pt complex **2** also smoothly reacts with H_2 and benzamide $PhCONH_2$ via oxidative addition of H−H and H−N bonds, respectively. The ensuing complexes **5** and **7** are stabilized by Pt−H→Al and Pt−NH−C(Ph) = O→Al bridging interactions, resulting in 5- and 7-membered metallacycles, respectively. DFT calculations have been performed in parallel with the experimental work. In particular, the mechanism of reaction of **2** with H_2 has been thoroughly analyzed, and the role of the Lewis acid moiety has been delineated. These results generalize the concept of constrained geometry TM→LA interactions and demonstrate the ability of Al-based ambiphilic ligands to participate in TM/LA cooperative reactivity. They extend the scope of small molecule substrates prone to such cooperative activation and contribute to improve our knowledge of the underlying factors.

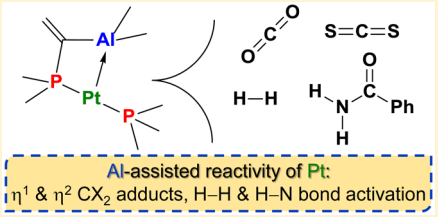

INTRODUCTION

The concept of Z-type ligands has considerably advanced over the past decade. The ability of Lewis acids (LA) to bind to transition metals (TM) as σ-acceptor ligands is now well-recognized and actually quite general in terms of the applied Lewis acid and transition metal.[1] Ambiphilic ligands with chelating assistance proved extremely fruitful to introduce Lewis acids in the coordination sphere, and to control the way they interact with the metal fragment.[2] The bonding situation associated with TM→LA interactions has attracted great interest.[3] In addition, the weak and electronically reverse nature of TM→LA interactions opens very interesting and unique possibilities in terms of reactivity.[2,4] In particular, a new type of metal/ligand cooperativity can be envisioned, involving a Lewis acid moiety instead of an electron-rich or redox-active site.[5] This approach has started to be explored recently, and a few complexes featuring TM→B interactions have been shown to promote cooperative activation of H−H and H−E bonds under stoichiometric or even catalytic conditions.[6,7] These first contributions are very promising and stimulate further investigations in this direction. In this context, we aimed in the present study: (*i*) to generalize the concept of constrained geometry TM→LA interactions recently introduced by Figueroa,[6e] (*ii*) to demonstrate the ability of Al-based ambiphilic ligands to participate in cooperative reactivity, and (*iii*) to extend the scope of TM/LA cooperativity to the formation of CX_2 adducts and to the activation of H−H as well as H−N bonds.

The prototypes of Z-type complexes and ambiphilic ligands are based on boranes, and so far, studies in the field have largely focused on boron-based Lewis acids. Replacing boron for aluminum is very appealing and should give rise to noticeably different properties, given the stronger and harder Lewis acid

Received: February 4, 2016
Published: March 15, 2016

DOI: 10.1021/jacs.6b01320
J. Am. Chem. Soc. 2016, 138, 4917−4926

Scheme 1. Synthesis and Structure of the PAl/Pt Complex 2[a]

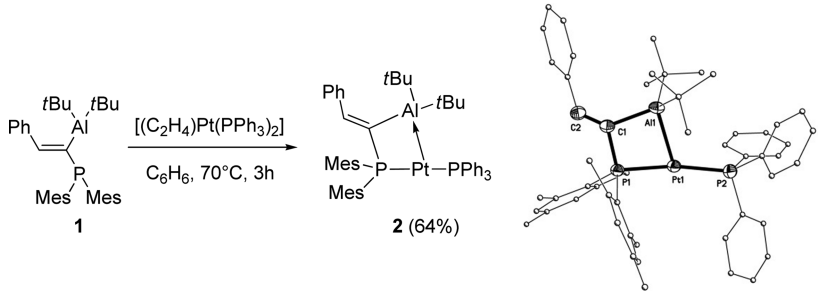

[a]The hydrogen atoms are omitted for clarity. Selected bond lengths (Å) and angles (deg) are as follows: Pt−P1, 2.2855(7); Pt1−P2, 2.2652(7); Pt1−Al1, 2.5610(8); Al1−C1, 2.057(3); C1−P1, 1.806(2); P1−Pt1−P2, 168.81(3); P1−Pt1−Al1, 74.02(3); P2−Pt1−Al1, 112.21(3); P1−C1−Al1, 98.3(1); C1−Al1−C31, 117.8(1); C31−Al1−C27, 117.8(1); C1−Al1−C27, 110.0(1).

character of Al compared to B. However, the number and variety of Al complexes are extremely limited.[1,8,9] Their reactivity has only rarely been explored, and so far, it is essentially restricted to the ionization of M−X bonds. This prompted us to investigate complexes of the geminal PAl compound [$Mes_2PC(=CHPh)Al tBu_2$] **1**. We recently reported the coordination of **1** to Rh, Pd, and Au.[8] In the ensuing complexes, the Al center interacts with or even abstracts a chloride at the metal (Rh and Pd), or binds to the metal (Au) as a Z-type ligand. Here we report a comprehensive study of a zerovalent Pt complex of **1**. It features a relatively strong Pt→Al interaction, but reacts with a range of small molecules (CO_2, CS_2, H_2, H_2NCOPh) via Pt/Al cooperativity.

RESULTS AND DISCUSSIONS

The geminal PAl ligand [$Mes_2PC(=CHPh)Al tBu_2$] (**1**) was reacted with [$(Ph_3P)_2Pt(H_2C=CH_2)$] in benzene for 3 h at 70 °C to afford after workup complex **2** as a yellow solid in 64% isolated yield (Scheme 1). The ^{31}P NMR spectrum of **2** shows two signals of equal intensities at δ 9.8 and 46.3 ppm, which are associated with the Mes_2P fragment of **1** and Ph_3P, respectively. Coordination of the PAl ligand to Pt is apparent from the large $^1J_{PtP}$ coupling constants (3244 and 3323 Hz, respectively), while the $^2J_{PP}$ coupling constant (345 Hz) is diagnostic of a *trans* arrangement of the two phosphines.[10] The olefinic proton of the PAl ligand in **2** displays a doublet at δ 7.58 ppm in the ^1H NMR spectrum with a large $^3J_{HP}$ coupling constant (48.1 Hz). This indicates quaternarization of both the P and Al atoms upon coordination of **1** to Pt,[8,11] and thus suggests the presence of a P→Pt→Al bridging interaction in **2**.

Crystals of **2** were grown from a saturated pentane solution at room temperature. X-ray diffraction analysis confirmed the κ^2-coordination of the PAl ligand (Scheme 1, right). The Pt center is three-coordinate and sits in a distorted T-shape environment. The $Mes_2P-Pt-PPh_3$ skeleton slightly deviates from linearity [168.81(3)°], while the $Mes_2P-Pt-Al$ and $Ph_3P-Pt-Al$ bond angles are different [74.02(3) and 112.21(3)°, respectively] due to the geometric constraints associated with the PAl ligand. The Pt−Al distance [2.5610(8) Å] is very close to the sum of the covalent radii (2.57 Å),[12] and the environment around Al is noticeably pyramidalized [sum of bond angles Σ(C−Al−C) = 346.6°, Al is displaced from the C_3 plane by 0.44 Å]. The four-membered PCAlPt metallacycle is almost planar (largest deviation from the mean plane <0.1 Å), and the PCAl moiety is strongly bent (98.3° vs 119.4° in the free ligand![11a]). All these geometric data support the presence of a significant Pt→Al interaction in complex **2**. Comparison with the few related systems is worthwhile (Chart 1):[13]

Chart 1. Structure and Key Structural Parameters of the Complexes I, II, III, and IV Related to 2 (*r* refers to the ratio between the M−LA distance and the sum of covalent radii)

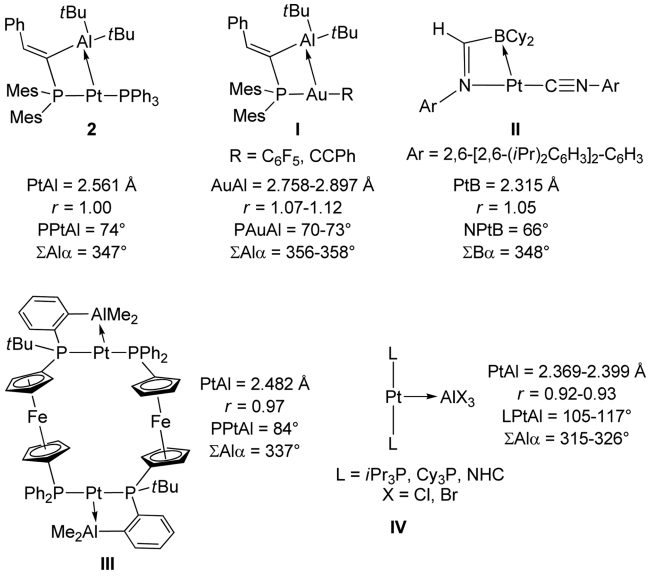

(i) The Pt→Al distance in **2** is significantly shorter than the Au→Al distances of the complexes **I** obtained by coordination of **1** to gold,[8b] which suggests a stronger TM→LA interaction in **2**, in line with the higher Lewis basicity of Pt vs Au.

(ii) Figueroa reported a Pt(0) complex **II** with an imine-borane ligand (N=C−B) and observed a significant Pt→B interaction.[6e] In this case, the PtB distance slightly exceeds the sum of covalent radii (by 5%) and the NPtB bite angle is even more acute (66.0°).

(iii) Emslie coordinated a 1,1′-diphosphinoferrocene with a lateral Al center (PPAl) to Pt complex **III** and characterized a dinuclear species with strong Pt→Al interactions.[6f] The geometry at Pt is close to T-shape (PPtAl = 84°), and the PtAl distance (2.482 Å) is shorter than in **2** due to reduced steric shielding around Al and formation of a 5- instead of 4-membered metallacycle.

(iv) Braunschweig prepared a series of Pt→AlX_3 complexes **IV** (X = Cl, Br),[14] which feature stronger Pt→Al

DOI: 10.1021/jacs.6b01320
J. Am. Chem. Soc. 2016, 138, 4917−4926

interactions, in line with the higher Lewis acidity of the Al atom and the absence of geometric constraints.

In order to get further insight into the nature of the Pt→Al interaction in **2**, a theoretical study was carried out at the ω-B97X-D/6-31G** level of theory[15] (Def2-TZVP and associated core potential for **Pt**, 6-31G** for all non−metallic atoms, 6-311+G** for the hydrogens involved in the reaction) using the Gaussian09 suite of software.[16] The influence of solvation (dichloromethane) has been taken into account in the reported Gibbs energies, using the PCM/SMD model implemented in Gaussian. First, the open and closed forms of the PAl platinum complex **2** were optimized (Scheme 2). It was

Scheme 2. Computed Structures for 2 and 2-open

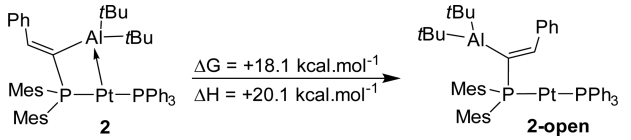

found that the closed form is more stable by 18.1 kcal mol^{-1} (ΔH = 20.1 kcal mol^{-1}), confirming our experimental observations of a Pt→Al interaction. To gain more insight, we performed second-order perturbation NBO analyses that confirmed the presence of a Pt→Al donor−acceptor interaction between a filled Pt(5d) orbital and an empty Al(3p) orbital (Figure 1). The TM→Al interaction is much stronger in **2** than in related Au complexes (see the Supporting Information),[8b] for which the energy difference between the open and closed forms is only 6.7−9.1 kcal mol^{-1}.

Next, we studied the reactivity of the Pt→Al complex **2** toward small molecules. The importance of carbon dioxide fixation and transformation at transition metals[17] prompted us to test the reaction of **2** with CO_2 first. A smooth reaction occurs at room temperature under 1 bar (Scheme 3). Conversion is complete after 17 h, and a new complex **3** is formed (85% spectroscopic yield). The reaction is irreversible. Complex **3** does not convert back to **2**, but it slowly decomposes both in vacuum and in solution into unidentified products (~15% decomposition after 10 h). Yet, it could be isolated with a yield of 45% as a white solid upon precipitation. The large $^2J_{PP}$ coupling constant (312 Hz) observed between the two ^{31}P NMR signals at δ 28.1 and 31.9 ppm indicates that the two phosphines remain *trans* in **3** ($^1J_{PPt}$ = 3279 and 3274 Hz). The ^{1}H NMR spectrum confirms the integrity of the PAl ligand and displays the olefinic proton at δ 7.13 ppm, again with a large $^3J_{HP}$ coupling constant (33.8 Hz). Besides the characteristic signals for the PAl ligand and PPh_3, the ^{13}C NMR spectrum also shows a doublet of doublets at δ 136.9 ppm with small J_{CP} coupling constants (4.4 and 3.3 Hz). Based on ^{13}C labeling studies (using $^{13}CO_2$), this signal can be unambiguously assigned to coordinated CO_2 and the direct Pt−CO_2 connectivity can be inferred from the presence of a large $^1J_{CPt}$ coupling constant (1258 Hz). Colorless crystals of **3** were obtained from a THF/pentane solution at −20 °C.[18] The X-ray diffraction analysis revealed CO_2 insertion into the Pt−Al bond (Scheme 3, right), resulting in a T-shape Pt complex. The two phosphines are in *trans* arrangement [P−Pt−P 176.46(8)°], and CO_2 is coordinated perpendicularly [Mes_2P−Pt−C and Ph_3P−Pt−C: 91.0(3) and 92.0(3)°, respectively]. The CO_2 molecule is bent [O−C−O 122.9(9)°] and rotated by 52.1° from the Pt coordination plane. Only the carbon atom is bonded to Pt [Pt−C 1.96(1) Å]; the CO_2 molecule is η^1-coordinated. One of the oxygen atoms interacts with the aluminum center [O−Al 1.833(7) Å], resulting in a 6-membered metallacycle. The corresponding C−O bond is elongated [1.30(1) vs 1.22(1) Å], and the environment around Al is pyramidal [Σ(C−Al−C) = 347°, Al is displaced from the C_3 plane by 0.42 Å]. Note that the fourth coordination site of Pt (*trans* to CO_2) is engaged in a δ agostic interaction with one of the *ortho*-Me groups of the Mes_2P moiety. The corresponding Pt···C and Pt···H distances [2.69(1) and 2.0417 Å, respectively] and the Pt···H−C bond angle [121.7°] fall in the same range than those reported for three-coordinate Pt(II) complexes featuring agostic interactions.[19,20] Low temperature ^{1}H and ^{13}C NMR analyses of **3** suggest that the agostic interaction is also present in solution.[21]

To further characterize this unique CO_2 complex, we again resorted to DFT calculations and found that the reaction of the masked Pt,Al-based FLP **2** with CO_2 to generate the T-shape Pt complex **3** is exergonic by 5.5 kcal mol^{-1} (ΔH = −11.3 kcal mol^{-1}). The computed structure of **3** (Figure 2, left) reproduced all the structural features of the X-ray structure, including the almost linear P−Pt−P angle (178.1°), the out-of-plane coordinated CO_2 moiety (63.3°), as well as the agostic interaction with a neighboring methyl group (Pt···H 2.167 Å). The corresponding C−H bond is slightly elongated (1.111 vs 1.093−1.095 Å). Interestingly, **3** is 5.0 kcal mol^{-1} (ΔH = 1.8 kcal mol^{-1}) more stable than its isomer **3′** (Figure 2, middle), which features a slightly bent P−Pt−P angle (164.2°), an in-plane coordinated CO_2 fragment (15.8°), and no agostic interaction. The η^2-coordinated CO_2 complex **3-η^2**, which has the two phosphines in a *cis* arrangement (110.9°; Figure 2,

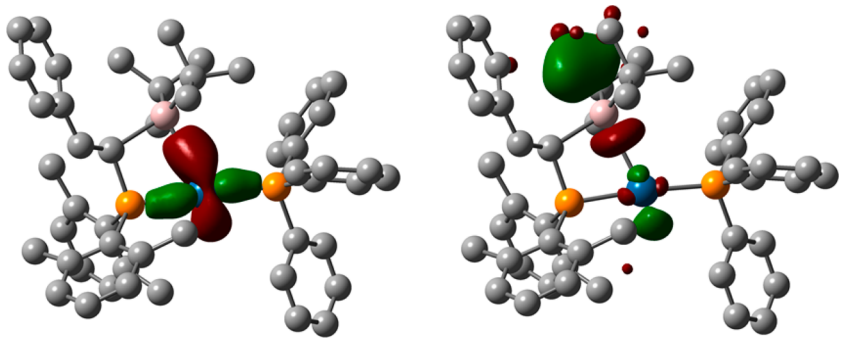

Figure 1. Donor (left) and acceptor (right) NBO orbitals involved in the Pt(5d)→Al(3p) interaction of **2** (isovalue: 0.06). H atoms have been omitted for clarity.

DOI: 10.1021/jacs.6b01320
J. Am. Chem. Soc. 2016, 138, 4917−4926

Scheme 3. Reaction of the Pt→Al Complex 2 with CO_2 and Molecular Structure of the Resulting η^1-CO_2 Complex 3[a]

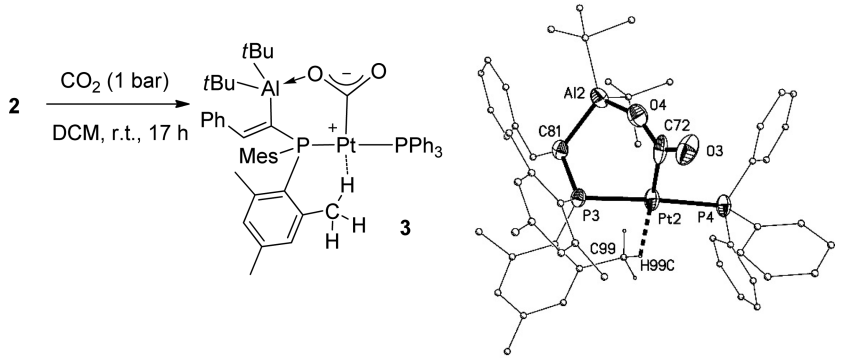

[a]The Mes, *t*Bu, and Ph groups are simplified, and the hydrogen atoms and solvate molecules are omitted for clarity. Selected bond lengths (Å) and angles (deg) are as follows: Pt–P3 2.326(2), Pt–P4 2.316(2), Pt–C72 1.96(1), C72–O3 1.22(1), C72–O4 1.30(1), Al–O4 1.833(7), P3–Pt–P4 176.46(8), P3–Pt–C72 91.0(3), P4–Pt–C72 92.0(3), Pt–C72–O4 116.0(7), Pt–C72–O3 121.0(7), O3–C72–O4 122.9(9).

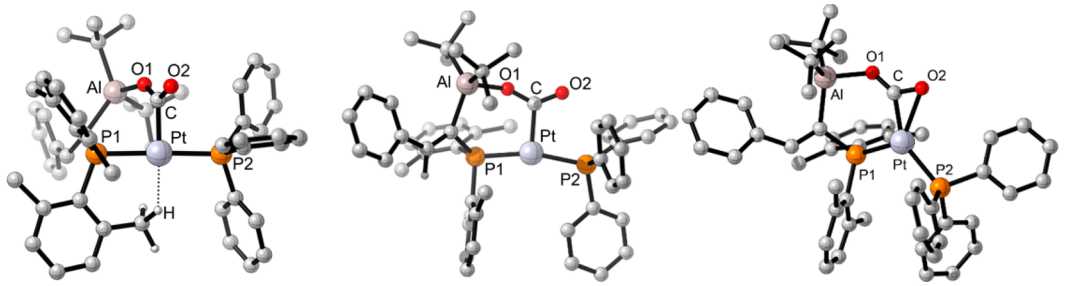

Figure 2. Optimized structures for **3** (left), **3′** (middle), and **3-η^2** (right). Selected bond distances (Å) and angles (deg) for **3**: Pt–P1 2.357, Pt–P2 2.333, Pt–C 2.006, Pt–H 2.167, C–O1 1.275, C–O2 1.213, Al–O1 1.883; P1–Pt–P2 178.1, C–Pt–H 167.6, P1–Pt–C 89.8, P2–Pt–C 92.1, Pt–C–O2 118.8, Pt–C–O1 112.5, O1–C–O2 128.7, C–O1–Al 143.1; **3′**: Pt–P1 2.329, Pt–P2 2.346, Pt–C 2.032, C–O1 1.270, C–O2 1.214, Al–O1 1.894; P1–Pt–P2 164.2, P1–Pt–C 98.0, P2–Pt–C 97.0, Pt–C–O2 115.4, Pt–C–O1 114.7, O1–C–O2 129.8, C–O1–Al 142.5; **3–η^2**: Pt–P1 2.264, Pt–P2 2.412, Pt–C 1.949, Pt–O2 2.293, C–O1 1.248, C–O2 1.247, Al–O1 1.915; P1–Pt–P2 110.9, P1–Pt–C 98.3, P2–Pt–O2 117.8, C–Pt–O2 32.9, Pt–C–O1 139.6, Pt–C–O2 117.8, O1–C–O2 131.5, C–O1–Al 127.1.

Scheme 4. Reaction of the Pt→Al Complex 2 with CS_2, and Molecular Structure of the Resulting η^2 Complex 4[a]

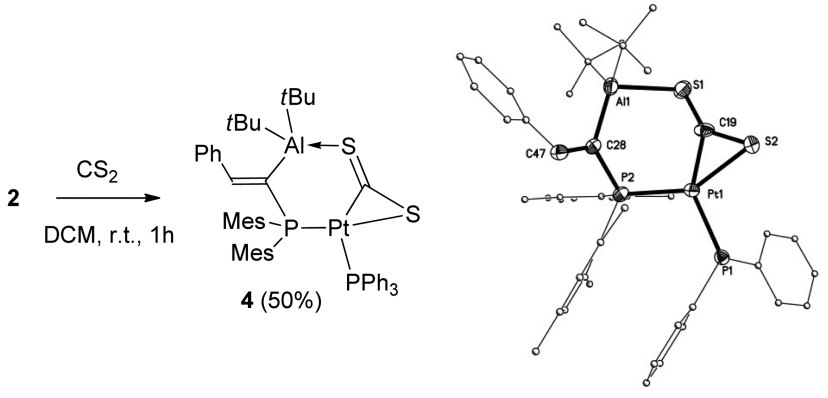

[a]The Mes, *t*Bu, and Ph groups are simplified, and the hydrogen atoms and solvate molecules are omitted for clarity. Selected bond lengths (Å) and angles (deg) are as follows: P1–Pt1 2.346 (1), P2–Pt1 2.289(1), Pt1–C19 1.984(5), Pt1–S2 2.384(1), S2–C19 1.619(6), S1–C19 1.670(5), S1–Al1 2.446(2); P1–Pt1–P2 111.24(4), C19–Pt1–S2 42.3(2).

right), could also be located on the potential energy surface, but it is the least stable isomer (ΔG = 12.8, ΔH = 6.6 kcal mol^{-1}). The stabilization energy associated with the agostic interaction in **3** was estimated to be ~1.2 kcal mol^{-1} in G by computing the fixation of CO_2 to a related PAl Pt complex featuring phenyl instead of mesityl groups at P (see Supporting Information).

The coordination and activation of CO_2 at transition metals has attracted huge interest over the last decades.[17] Most CO_2 complexes adopt η^2-CO_2 coordination, but η^1-CO_2 coordination has also been observed occasionally.[22,23] Compared with the other transition metals, relatively little is known about CO_2 complexes of the group 10 metals. Some Ni complexes have been structurally authenticated,[24] while a few Pd complexes have been characterized spectroscopically.[25] The T-shape η^1-structure of **3** is unique and takes advantage of the Lewis acid center, which favors the bridging coordination of CO_2 between Pt and Al, resulting in a 6-membered metallacycle. The

DOI: 10.1021/jacs.6b01320
J. Am. Chem. Soc. 2016, 138, 4917–4926

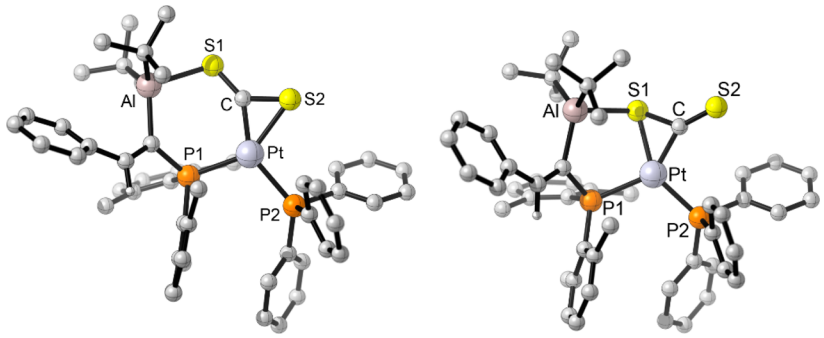

Figure 3. Optimized structures for **4** (left) and **4′** (right). Selected bond lengths (Å), bond and torsion angles (deg) for **4**: Pt−P1 2.328, Pt−P2 2.414, Pt−C 1.977, Pt−S2 2.390, C−S1 1.650, C−S2 1.682, Al−S1 2.451; P1−Pt−P2 111.3, P1−Pt−C 102.3, C−Pt−S2 44.1, P2−Pt−S2 102.4, S2−C−Pt 81.1, C−S2−Pt 54.8, S1−C−S2 134.6, Pt−C−S1 143.8, C−S1−Al 108.9; Pt−P1−Al−S1 22.0, P1−P2−S2−C 3.1; **4′**: Pt−P1 2.444, Pt−P2 2.294, Pt−C 1.979, C−S1 1.767, C−S2 1.611, Al−S1 2.538; P1−Pt−P2 114.0, P1−Pt−C 141.6, P2−Pt−C 102.5, Pt−C−S1 78.1, Pt−C−S2 145.6, S1−C−S2 136.2, C−S1−Al 122.8; Pt−P1−Al−S1 25.0, P1−P2−S1−S2 24.4.

Scheme 5. Activation of H_2 by the PAl/Pt Complex 2 and Computed Structure of the Resulting Pt Complex 5[a]

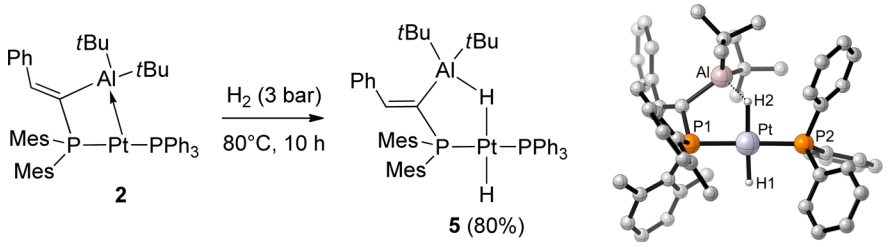

[a]Selected bond lengths (Å) and angles (deg) for **5**: P1−Pt 2.345, Pt−P2 2.297, Al−H2 1.798, Pt−H2 1.698, Pt−H1 1.598; P1−Pt−P2 173.5, H1−Pt−H2 176.6, Al−H2−Pt 118.4.

presence of the agostic interaction is also noteworthy, and complex **3** is a rare example of a masked three-coordinate T-shape Pt complex.[19,20]

Next, the reaction of Pt→Al complex **2** with carbon disulfide was investigated.[17a,24c,26] The new complex **4** was obtained within 1 h upon stirring **2** with 5 equiv of CS_2 at room temperature (Scheme 4). The ^{31}P NMR spectrum shows two doublets at δ 12.3 and 17.3 ppm (J_{PPt} = 4803 and 3086 Hz, respectively) with, in marked contrast to **2** and its CO_2 complex **3**, a small J_{PP} coupling constant (16.8 Hz), indicating a *cis* arrangement of the two phosphines. The carbon atom of the coordinated CS_2 molecule appears at low field in the ^{13}C NMR spectrum (δ 262.1 ppm) with two very different J_{CP} coupling constants (2.4 and 79.6 Hz), suggesting a nonsymmetric coordination to Pt. Here also the direct connection between Pt and CS_2 was deduced from ^{13}C labeling. Using $^{13}CS_2$, the Pt satellites could be observed in the ^{13}C NMR spectrum and a large $^1J_{CPt}$ coupling constant was measured (615 Hz). Like in the CO_2 case, fixation of CS_2 is irreversible and complex **4** does not evolve back to **2** in vacuum. Orange-red crystals of **4** were obtained from a dichloromethane/pentane solution at −20 °C. The X-ray diffraction analysis confirmed CS_2 insertion into the Pt−Al bond (Scheme 4, right) and revealed a distorted Y-shape structure with an in-plane coordinated CS_2 moiety that is strongly bent [SCS = 137.7(6)°]. As indicated by ^{31}P NMR spectroscopy, the Mes_2P−Pt−PPh_3 framework deviates significantly from linearity [111.24(4)°]. The CS_2 fragment is η^2-coordinated, with one sulfur atom connected to Pt and the other one interacting with the Al center. The corresponding AlS bond is relatively short [2.446(2) Å],[27] the environment around Al is pyramidal [Σ(C−Al−C) = 351°, Al is displaced from the C_3 plane by 0.37 Å], and the CS bond is slightly elongated [1.670(5) vs 1.619(6) Å]. Complex **4** is a rare example of a Pt−CS_2 complex.[26a,28] Its structure differs from those of other complexes by the interaction of the exocyclic S atom with Al, leading to fused 6- and 3-membered metallacycles.

Also in this case, DFT calculations provided additional insight. The reaction of the masked Pt,Al-based FLP **2** with CS_2 to generate the experimentally ascertained structure **4** (Figure 3, left) is exergonic by 2.7 kcal mol^{-1} (ΔH = −17.2 kcal mol^{-1}). In this case, only one other isomer could be found (**4′**; Figure 3, right), which is slightly higher in energy (ΔG = 0.6, ΔH = 0.9 kcal mol^{-1}) and features fused 5- and 3-membered metallacycles with an exocyclic C═S double bond. The interconversion between 4 and 4′ involves a relatively large energy barrier ($\Delta G^{\ddagger}$ 16.9, $\Delta H^{\ddagger}$ 20.0 kcal mol^{-1}). No η^1-coordinated CS_2 complex could be optimized, and the corresponding calculations converged rapidly to **4**.

Formally, CO_2 and CS_2 react with complex **2** by insertion into the Pt→Al bond. The electron-rich Pt center attacks the electrophilic carbon atom while the Al center stabilizes the extra electron density at O/S. We were then interested to study the activation of σ-bonds across the Pt→Al interaction of **2** and first investigated its reaction with dihydrogen. Oxidative addition of H_2 across M→B interactions (M = Ni, Co, Pt) has been recently reported by Peters, Figueroa, and Emslie using PBP, NB, and PPB ambiphilic ligands, respectively.[6b−g] The Pt→Al complex **2** cleanly and quantitatively reacts with H_2 at 80 °C and 3 bar (Scheme 5). The resulting complex **5** resonates as an AB system in the ^{31}P NMR spectrum (δ −17.3 and 28.4 ppm). The large $^2J_{PP}$ coupling constant (364 Hz) indicates the retention of the *trans* arrangement of the two phosphines, while the $^1J_{PPt}$ coupling constants significantly decrease from **2** to **5**

DOI: 10.1021/jacs.6b01320
J. Am. Chem. Soc. 2016, 138, 4917−4926

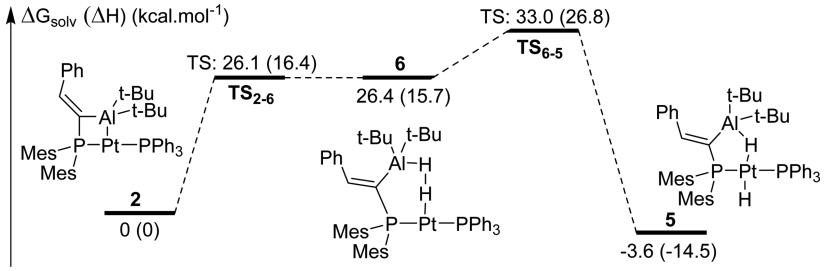

Figure 4. Mechanism for Al-assisted activation of H_2 by Pt→Al complex **2** at 353 K.

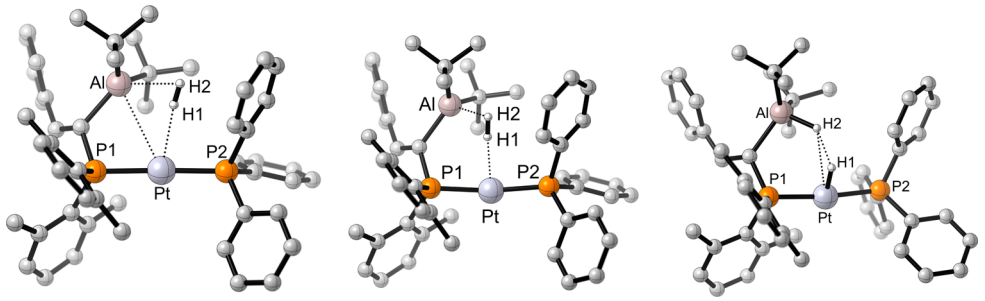

Figure 5. Optimized structures of $\mathbf{TS}_{2-6}$ (left), **6** (middle), and $\mathbf{TS}_{6-5}$ (right). Selected bond lengths (Å) and angles (deg) for $\mathbf{TS}_{2-6}$: P1−Pt 2.322, Pt−P2 2.270, Al−H2 2.485, H1−H2 0.757, Pt−H1 2.395, Al−Pt 3.416; P1−Pt−P2 173.2, Pt−H1−H2 170.1, Al−Pt−H1 44.1, Al−H2−H1 73.1; for **6**: P1−Pt 2.339, Pt−P2 2.254, Al−H2 1.954, H1−H2 0.791, Pt−H1 2.109; P1−Pt−P2 168.9, Pt−H1−H2 171.11, Al−Pt−H1 29.0, Al−H2−H1 92.0; for $\mathbf{TS}_{6-5}$: P1−Pt 2.346, Pt−P2 2.309, Al−H2 1.654, H1−H2 1.635, Pt−H1 1.525; P1−Pt−P2 174.1, Pt−H1−H2 130.9, Al−H2−H1 129.5, H1−Pt−H2 25.5.

Scheme 6. Reaction of Benzamide with the Pt→Al Complex 2 *via* N−H Bond Activation[a]

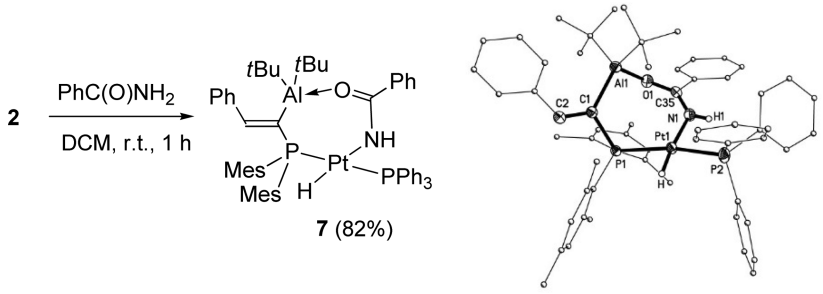

[a]Molecular structure of the resulting complex **7**. The Mes, *t*Bu, and Ph groups are simplified, the hydrogen atoms and solvate molecules are omitted for clarity. Selected bond lengths (Å) and angles (deg) are as follows: P1−Pt1 2.340(1), P2−Pt1 2.259(2), Pt1−N1 2.097(5), Pt1−H 1.41(4); P1−Pt1−P2 167.56(5), N1−Pt1−H 174(1).

(from 3244/3323 Hz to 2717/2662 Hz), in line with Pt(0) → Pt(II) oxidation.[29] The ^{1}H NMR spectrum shows two hydridic signals at δ −3.54 and −8.64 ppm with a large $^2J_{HH}$ coupling constant (20.2 Hz), indicative of a dissymmetric *trans* Pt dihydride moiety. This pattern results from the interaction of one Pt hydride with the Al center (Pt−H−Al bridging coordination). A similar situation was observed for H_2 activation by PPB and NB complexes of Ni and Pt.[6b−e] The bridging hydride resonates at lower field (δ −3.54 ppm in the case of **5**, $\Delta\delta$ = 5.1 ppm), and the corresponding $^1J_{PtH}$ coupling constant is significantly smaller (691 vs 1023 Hz), in line with a weakening of the Pt−H bond. Finally, the $^2J_{HP}$ coupling constants involving the $PMes_2$ and PPh_3 fragments were resolved by selective ^{31}P decouplings. The NMR data unambiguously established the structure of **5** as a *trans* hydrido-aluminohydride Pt(II) complex, which is formed by oxidative addition of dihydrogen to Pt and formal insertion of one of the hydrides into the Pt→Al bond. No sign of H_2 release was observed even when **5** was exposed to dynamic vacuum, meaning that the oxidative addition is irreversible. Complex **5** was isolated as a pale yellow powder in 80% yield. In the absence of crystallographic characterization (despite strong efforts, no crystals of X-ray quality could be obtained), its structure was analyzed by DFT calculations (Scheme 5, right), which shows a square planar hydrido−aluminohydride complex with two *trans*-phosphine donors, a terminal Pt−H bond, and a hydride ligand bridging Al and Pt.

To shed light on the role of the Lewis acid moiety in this H_2 activation process, the mechanism of formation of the Pt dihydride **5** was studied by DFT calculations, which revealed some interesting features (Figures 4 and 5). First, dihydrogen is trapped by complex **2** via insertion into the Pt→Al bond, creating **6** (ΔG^{353} = 26.4, ΔH^{353} = 15.7 kcal mol^{-1}), in which H_2 is end-on coordinated to Pt and side-on coordinated to Al (Figure 5, middle). Intermediate **6** is formed via a late transition state $\mathbf{TS}_{2-6}$ ($\Delta G^{\ddagger 353}$ = 26.1, $\Delta H^{\ddagger 353}$ = 16.4 kcal mol^{-1}), which clearly illustrates the cooperative Pt,Al-based activation of dihydrogen (Figure 5, left). In this process, the H_2

DOI: 10.1021/jacs.6b01320
J. Am. Chem. Soc. 2016, 138, 4917−4926

molecule is elongated, going from 0.744 Å in the free form, to 0.757 Å in $\mathbf{TS_{2-6}}$, and 0.791 Å in intermediate **6**. Subsequently, the H−H bond breaks and **6** converts into product **5** ($\Delta\Delta G^{353}$ = −30.0, $\Delta\Delta H^{353}$ = −30.2 kcal mol^{-1}) via $\mathbf{TS_{6-5}}$ ($\Delta\Delta G^{\ddagger 353}$ = 6.6, $\Delta\Delta H^{\ddagger 353}$ = 11.1 kcal mol^{-1}; H1−H2 1.635 Å). Along this process, H2 remains bound to Al and gradually approaches Pt, while H1 is moving toward the *trans* position. According to NBO charges, the H_2 molecule is slightly polarized in **6**: +0.08 for H1/−0.08 for H2. H1 remains slightly positively charged in $\mathbf{TS_{6-5}}$ (+0.13) while H2 acquires strong hydridic character (−0.52).

While the overall energetic span is rather high (but not incompatible with the applied reaction conditions), each step is facilitated by stabilizing interactions with the Lewis acidic aluminum moiety (see Supporting Information for the corresponding non-Al-assisted reaction pathway).

The ability of complex **2** to split dihydrogen and the active participation of the Lewis acid moiety prompted us to explore the reaction of a polar X−H bond. To this end, 1 equiv of benzamide $PhCONH_2$ was added to a dichloromethane solution of **2**. Within 1 h at room temperature, a new complex **7** was obtained (Scheme 6). The ^{31}P NMR data are diagnostic of a *trans* Pt(II) complex with an AB spin system at δ 12.6 and 26.9 ppm, with a large J_{PP} coupling constant (385 Hz) and J_{PtP} coupling constants of 2999 and 2890 Hz, respectively. The ^{1}H NMR spectrum displays a Pt−H signal at δ −16.4 ppm (dd, small J_{HP} couplings of 11.8 and 17.0 Hz, $^1J_{HPt}$ = 965.8 Hz) and a broad signal integrating for 1 H at δ 5.8 ppm attributable to the N*H*COPh moiety. Crystals of **7** were obtained from a dichloromethane/pentane solution at −20 °C, and an X-ray diffraction study was performed (Scheme 6, right). The Pt center is in a square-planar environment with the two phosphines in *trans* position [PPtP = 167.56(5)°]. The hydride at Pt was unambiguously located in the difference Fourier map, with a rather short Pt−H distance of 1.41(4) Å.[30] The NHC(O)Ph amide fragment bridges the Pt and Al centers. The N atom is bonded to Pt, and the O atom strongly interacts with Al, as apparent from the short OAl distance [1.826(3) Å] and the noticeable pyramidalization of Al [Σ(C−Al−C) = 346.3°, Al deviates from the C_3 plane by 0.44 Å]. Thus, complex **7** results from the oxidative addition of one N−H bond of benzamide to Pt with formal insertion of the NHC(O)Ph moiety into the Pt→Al bond. The process is reminiscent of that observed upon reacting the imino−borane Pt complex (see Chart S1, SI) with anilines and phenols.[6e] However, the formation of a 7-membered metallacycle by a Pt−NH−C(Ph)═O→Al bridging interaction is remarkable and contrasts with the Pt−N/O→B interactions (and 5-membered rings) observed by Figueroa. It is also striking to note that the free PAl ligand was shown to readily react with benzamide and protonolysis of the $C_{sp}2$−Al bond was observed.[11d] Thus, the ambiphilic PAl ligand is protected by coordination to Pt, and it actually plays a major role in the activation of benzamide by **2**, as demonstrated by control experiments with Lewis acid-free Pt complexes. Indeed, under similar conditions, no reaction was observed when $[Pt(PPh_3)_2(H_2C{=}CH_2)]$ or $[Pt(PCy_3)_2]$ was treated with benzamide. Oxidative addition of amide N−H bonds to Pt is in fact very uncommon.[31]

CONCLUSION

In summary, the Pt(0) complex **2** was readily prepared by reaction of the geminal PAl ligand **1** with $[Pt(PPh_3)_2(ethylene)]$. NMR and XRD data, as well as DFT calculations, indicate the presence of a significant Pt→Al interaction. Complex **2**, which can be considered as a unimolecular metal-only Lewis pair,[32] displays rich reactivity. It forms the unique T-shape η^1-adduct **3** with CO_2 and gives the bent η^2-complex **4** with CS_2, which are stabilized by O,S→Al interactions. Complex **2** also reacts smoothly with H_2 and $PhCONH_2$ via oxidative addition of the H−H and N−H bonds to Pt. The ensuing Pt complexes **5** and **7** are stabilized by Pt−H→Al and Pt−NH−C(Ph)═O→Al bridging interactions. These results demonstrate the ability of Al-containing ambiphilic ligands to participate in TM/LA cooperative reactivity and extend the scope of small molecule substrates prone to such cooperativity (see Chart 2). In addition, the

Chart 2. Schematic Representation of the Borane Complexes Displaying TM/LA Cooperativity and Associated Small Molecule Substrates[a]

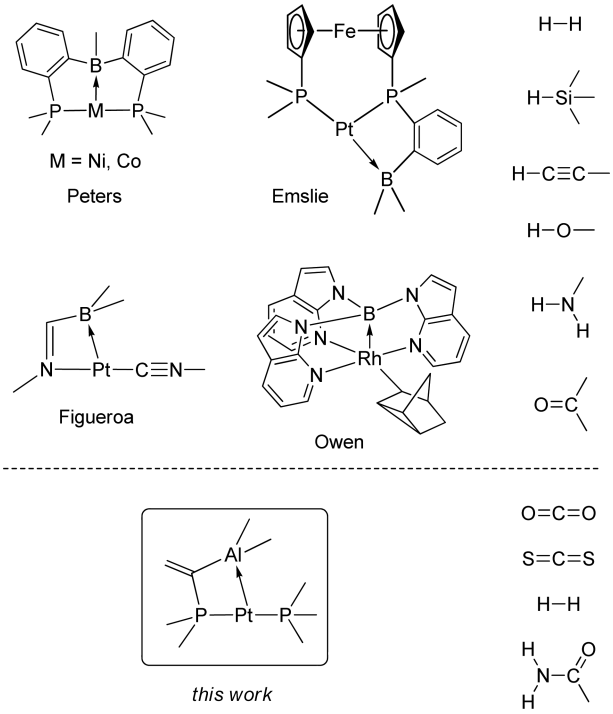

[a]PAl Pt complex studied in this work and compounds engaged in Pt/Al cooperative reactivity.

mechanistic study carried out on the activation of H_2 provides useful information on the role and mode of action of the Lewis acid moiety. The resulting Pt−H→Al interaction is an important driving force and the Al center assists the oxidative addition of H_2 to Pt. So far, mechanistic studies on TM/LA cooperativity remain extremely scarce, and very little is known on the role of LA in such reactions. The results obtained here with the PAl/Pt complex **2** are hardly comparable with those reported recently by Peters and Sakaki for PBP/Ni complexes[6b−d] (the metal, the Lewis acid, the denticity, and the framework of the ligand are different). Nonetheless, they extend the variety of systems displaying TM/LA cooperativity in small molecule activation. They also contribute to improve our knowledge of the underlying factors.

Of note, the reactivity of the Pt complex **2** completes and goes beyond that of the free ligand. The PAl compound **1** forms a cyclic P−C/Al−O adduct with CO_2,[11a] while the Pt complex **2** gives a unique T-shape η^1-CO_2 adduct stabilized by

DOI: 10.1021/jacs.6b01320
J. Am. Chem. Soc. 2016, 138, 4917−4926

O→Al interaction. Moreover, the free ligand does not react with H_2[11a] and undergoes C−Al cleavage with benzamide,[11d] while H−H and H−N bond activations with cleavage of the Pt→Al interaction are observed with **2**. It is also important to note that the geminal PAl ligand **1** has quite unique features. The strain generated upon its coordination to Pt does not prevent the formation of a significant Pt→Al interaction in **2**. Meanwhile, it enables rich reactivity across the Pt→Al interaction and the Al center shows versatile ability to stabilize the ensuing complexes, via O,S→Al or Pt−H→Al interactions, with formation of 5-, 6-, or even 7-membered metallacycles. Future work from our groups will seek to develop further the reactivity of TM→Al complexes. We will particularly endeavor to exploit the strong affinity of Al for electronegative elements such as oxygen to mediate challenging transformations.

EXPERIMENTAL SECTION

General Comments. All reactions and manipulations were carried out under an atmosphere of dry argon using standard Schlenk techniques. All solvents were sparged with argon and dried using an MBRAUN Solvent Purification System (SPS). ^{1}H, ^{13}C, and ^{31}P NMR spectra were recorded on a Bruker Avance 500 or 300 spectrometers. Chemical shifts are expressed with a positive sign, in parts per million, calibrated to residual ^{1}H (7.24 ppm) and ^{13}C (77.16 ppm) solvent signals and 85% H_3PO_4 (0 ppm), respectively. Otherwise stated, NMR spectra were recorded at 293 K. Mass spectra were recorded on a Waters LCT mass spectrometer. The phosphine-alane ligand Mes_2P-(C═CHPh)Al*t*Bu_2 **1** was prepared as previously described.[11a] In the NMR assignment, the Ph group at C is denoted Ar, the ones at P are denoted Ar′ and the one on the amide in **7** is denoted Ar″.

Complex 2. A solution of **1** (50 mg, 0.098 mmol) and bis(triphenylphosphine) ethylene platinum (0) (72.9 mg, 0.098 mmol, 1 equiv) in benzene (1 mL) was heated at 70 °C for 3h. The volatiles were then removed under vacuum and the crude mixture was extracted with pentane (5 mL) at room temperature. The expected product **2** was precipitated from the pentane solution at −60 °C in 64% yield. Yellow crystals suitable for X-ray diffraction analysis were obtained from a saturated solution in pentane at room temperature. ^{1}H NMR (500 MHz, 20 °C, C_6D_6, δ): 1.36 (s, 18H, *t*Bu), 2.20 (s, 6H, $CH_{3p\text{-}Mes}$), 2.98 (s, 12H, $CH_{3o\text{-}Mes}$), 6.85 (d, 4H, $^{4}J_{HP}$ = 2.9 Hz, $H_{m\text{-}Mes}$), 7.12−7.19 (m, 8H, $H_{arom.}$), 7.24−7.30 (m, 5H, $H_{arom.}$), 7.58 (d, 1H, $^{3}J_{HP}$ = 48.1 Hz, HCCP), 7.80 (m, 2H, $H_{arom.}$), 7.86−7.93 (m, 5H, $H_{arom.}$). ^{13}C{^{1}H} NMR (126 MHz, 20 °C, C_6D_6, δ): 20.5 (s br., 2C, Al(C(CH$_3$)$_3$)$_2$), 20.9 (s, 2C, $CH_{3p\text{-}Mes}$), 26.2 (d, 4C, $^{3}J_{CP}$ = 7.0 Hz, $CH_{3o\text{-}Mes}$), 33.2 (s, 6C, *t*Bu), 128.3 (s br., $CH_{p\text{-}Ar}$), 128.6 (d, 6C, J_{CP} = 10.0 Hz, $CH_{Ar'}$), 128.6 (s br., 2C, CH_{Ar}), 128.7 (s br., 2C, CH_{Ar}), 130.4 (dd, 2C, $^{1}J_{CP}$ = 37.9 Hz, $^{3}J_{CP}$ = 2.0 Hz, $C_{ipso\text{-}Mes}$), 130.5 (d, 3C, $^{4}J_{CP}$ = 2.0 Hz, $CH_{p\text{-}Ar'}$), 131.2 (d, 4C, $^{3}J_{CP}$ = 8.0 Hz, $CH_{m\text{-}Mes}$), 134.0 (dd, 3C, $^{1}J_{CP}$ = 45.4 Hz, $^{3}J_{CP}$ = 1.7 Hz, $C_{ipso\text{-}Ar'}$), 135.3 (d, 6C, J_{CP} = 12.9 Hz, $CH_{Ar'}$), 139.0 (d, 2C, $^{4}J_{CP}$ = 2.0 Hz, $C_{p\text{-}Mes}$), 142.4 (dd, 4C, $^{2}J_{CP}$ = 8.9 Hz, $^{4}J_{CP}$ = 1.4 Hz, $C_{o\text{-}Mes}$), 142.5 (d, $^{3}J_{CP}$ = 30.4 Hz, $C_{ipso\text{-}Ar}$), 149.0 (dd, $^{2}J_{CP}$ = 11.2 Hz, $^{4}J_{CP}$ = 3.7 Hz, HCCP), 154.0 (d, $^{1}J_{CP}$ = 30.4 Hz, HCCP). ^{31}P{^{1}H} NMR (202 MHz, 20 °C, C_6D_6, δ): 9.8 (d, $^{2}J_{PP}$ = 344.8 Hz, $^{1}J_{PPt}$ = 3243.9 Hz), 46.3 (d, $^{2}J_{PP}$ = 344.8 Hz, $^{1}J_{PPt}$ = 3323.0 Hz).

Complex 3. A pressure NMR tube containing a solution of **2** (20 mg, 0.021 mmol) in CD_2Cl_2 (0.4 mL) was loaded with carbon dioxide (1 bar) during 17h at r.t. The reaction was followed by ^{31}P{^{1}H} NMR. The compound could be isolated with a yield of 45% as a white powder by adding pentane (0.4 mL) to a concentrated solution of **3** in CD_2Cl_2. Colorless crystals were obtained by adding pentane (0.2 mL) to a concentrated solution of **3** in THF at −20 °C. For spectroscopic data of unlabeled **3**, see SI. Spectroscopic data for labeled **3*** prepared by the same procedure are described hereafter. ^{1}H NMR (400 MHz, −40 °C, CD_2Cl_2, δ): 0.70 (s br., 18H, *t*Bu), 2.24 (m, 18H, $CH_{3p\text{-}Mes}$ and $CH_{3o\text{-}Mes}$), 6.83 (s br., 4H, $H_{m\text{-}Mes}$), 7.04 (dd, J_{HP} = 8.8 Hz, J_{HP} = 34.6 Hz, HCCP), 7.24 (d, 1H, $^{3}J_{HH}$ = 6.9 Hz, $CH_{p\text{-}Ar}$), 7.30 (t, 2H, $^{3}J_{HH}$ = 7.1 Hz, CH_{Ar}), 7.38 (m, 2H, CH_{Ar}), 7.46 (m, 9H, $CH_{Ar'}$), 7.57 (m, 6H, $CH_{Ar'}$). ^{13}C{^{1}H} NMR (101 MHz, − 40 °C, CD_2Cl_2, δ): 16.9 (s br., 2C, Al(C(CH$_3$)$_3$)$_2$), 20.8 (s, 4C, $CH_{3o\text{-}Mes}$), 23.0 (s br., 2C, $CH_{3p\text{-}Mes}$), 33.2 (s, 6C, *t*Bu), 127.8 (s, 1C, $CH_{p\text{-}Ar}$), 127.9 (s, 2C, $CH_{o\text{-}Ar}$), 128.6 (s, 2C, $CH_{m\text{-}Ar}$), 128.9 (dd, 6C, J_{CP} = 1.8 Hz, J_{CP} = 8.5 Hz, $CH_{Ar'}$), 130.2 (dd, 1C, J_{CP} = 12.4 Hz, J_{CP} = 40.2 Hz, C_{quat}), 130.9 (d, 1C, J_{CP} = 6.8 Hz, $CH_{m\text{-}Mes}$), 131.3 (s, 1C, $CH_{Ar'}$), 133.9 (dd, 1C, J_{CP} = 3.4 Hz, J_{CP} = 9.4 Hz, $CH_{Ar'}$), 136.9 (dd, $^{2}J_{CP}$ = 3.3 Hz, $^{2}J_{CP}$ = 4.4 Hz, $^{1}J_{CPt}$ = 1257.7 Hz, $^{13}CO_2$), 141.1 (s, 1C, C_{quat}), 141.8 (dd, 1C, J_{CP} = 6.5 Hz, J_{CP} = 23.4 Hz, C_{quat}), 142.4 (m, 1C, C_{quat}), 143.5 (d, 1C, J_{CP} = 8.6 Hz, C_{quat}), 146.5 (dd, 1C, J_{CP} = 6.0 Hz, J_{CP} = 28.4 Hz, C_{quat}), 147.9 (d, 1C, J_{CP} = 4.6 Hz, HCCP). ^{31}P{^{1}H} NMR (162 MHz, − 40 °C, CD_2Cl_2, δ): 27.5 (d, $^{2}J_{PP}$ = 312 Hz, $^{1}J_{PPt}$ = 3279.3 Hz, $^{2}J_{PC}$ = 4.4 Hz), 29.8 (d, $^{2}J_{PP}$ = 312 Hz, $^{1}J_{PPt}$ = 3273.6 Hz, $^{2}J_{PC}$ = 3.3 Hz).

Complex 4. A NMR tube containing a solution of **2** (20 mg, 0.021 mmol) in CD_2Cl_2 (0.4 mL) was loaded with carbon disulfide (6.5 μL, 0.105 mmol) and allowed to react during 1h at r.t. The solution was concentrated and pentane (0.4 mL) was added. The solution was placed at −20 °C for 10 h and the expected product precipitated. It was obtained as a yellow powder with a yield of 50% after filtration and removing of volatiles. Orange-red crystals were obtained by adding pentane (0.2 mL) to a concentrated solution of **4** in CD_2Cl_2 at −20 °C. The labeled complex **4*** was prepared following the same procedure by using labeled $^{13}CS_2$, and CD_2Cl_2. **4*** was not isolated and its purity was estimated to 90% by ^{31}P{^{1}H} NMR. **4*** was fully characterized by multinuclear NMR: ^{1}H NMR (500 MHz, − 80 °C, CD_2Cl_2, δ): 0.48 (s, 9H, *t*Bu), 0.52 (s, 9H, *t*Bu), 1.29 (s, 3H, $CH_{3o\text{-}Mes}$), 2.03 (s br., 3H, $CH_{3o\text{-}Mes}$), 2.12 (s, 3H, $CH_{3p\text{-}Mes}$), 2.20 (s, 3H, $CH_{3p\text{-}Mes}$), 2.48 (s, 3H, $CH_{3o\text{-}Mes}$), 3.03 (s br., 3H, $CH_{3o\text{-}Mes}$), 6.23 (s br., 1H, $H_{m\text{-}Mes}$), 6.35 (s br., 1H, $H_{m\text{-}Mes}$), 6.73 (s br., 1H, $H_{m\text{-}Mes}$), 6.85 (s br., 1H, $H_{m\text{-}Mes}$), 7.28 (m, 21H, CH_{Ar} and $CH_{Ar'}$ and HCCP). ^{13}C{^{1}H} NMR (125.7 MHz, − 80 °C, CD_2Cl_2, δ): 18.1 (s br., 1C, Al(C(CH$_3$)$_3$)$_2$), 19.3 (s br., 1C, Al(C(CH$_3$)$_3$)$_2$), 20.4 (s, 1C, $CH_{3p\text{-}Mes}$), 20.5 (s, 1C, $CH_{3p\text{-}Mes}$), 24.3 (s, 1C, $CH_{3o\text{-}Mes}$), 25.4 (s, 1C, $CH_{3o\text{-}Mes}$), 26.2 (d, 1C, $^{3}J_{CP}$ = 9.8 Hz, $CH_{3o\text{-}Mes}$), 29.2 (d, 1C, $^{3}J_{CP}$ = 11.6 Hz, $CH_{3o\text{-}Mes}$), 31.4 (s, 3C, $CH_{3\text{-}tBu}$), 31.7 (s, 3C, $CH_{3\text{-}tBu}$), 125.3 (d, 1C, J_{CP} = 33.8 Hz, C_{quat}), 126.7 (d, 1C, J_{CP} = 55.6 Hz, C_{quat}), 127.1 (s, CH_{Ar}), 128.1 (d, 6C, J_{CP} = 9.6 Hz, $CH_{Ar'}$), 128.2 (s, 3C, $CH_{Ar'}$), 128.4 (d, 1C, J_{CP} = 7.0 Hz, C_{quat}), 128.5 (s, CH_{Ar}), 129.8 (s, CH_{Ar}), 130.0 (d, 1C, J_{CP} = 7.4 Hz, $CH_{m\text{-}Mes}$), 130.8 (d, 1C, J_{CP} = 9.5 Hz, $CH_{m\text{-}Mes}$), 131.2 (d, 1C, J_{CP} = 6.1 Hz, $CH_{m\text{-}Mes}$), 131.5 (d, 1C, J_{CP} = 7.8 Hz, $CH_{m\text{-}Mes}$), 132.3 (d, 3C, J_{CP} = 44.2 Hz, $C_{ipso\text{-}Ar'}$), 133.6 (d, 6C, J_{CP} = 12.4 Hz, $CH_{Ar'}$), 138.2 (d, 1C, J_{CP} = 16.5 Hz, C_{Mes}), 138.5 (s br. 1C, C_{Mes}), 139.7 (s br., 1C, C_{Mes}), 140.6 (d, 1C, J_{CP} = 2.7 Hz, C_{Mes}), 141.8 (d, 1C, J_{CP} = 14.6 Hz, C_{Mes}), 142.0 (d, 1C, J_{CP} = 13.9 Hz, $C_{o\text{-}Mes}$), 145.1 (s br., 1C, $C_{o\text{-}Mes}$), 153.9 (d, J_{CP} = 7.7 Hz, HCCP), 262.1 (d br, 1C, $^{2}J_{CP}$ = 2.4 and 79.6 Hz, $^{1}J_{CPt}$ = 615.1 Hz, $^{13}CS_2$). ^{31}P{^{1}H} NMR (202 MHz, − 80 °C, CD_2Cl_2, δ): 12.3 (dd, $^{2}J_{PP}$ = 16.8 Hz, $^{2}J_{PC}$ = 2.4 Hz, $^{1}J_{PPt}$ = 4802.7 Hz), 17.3 (dd, $^{2}J_{PP}$ = 16.8 Hz, $^{2}J_{PC}$ = 79.6 Hz, $^{1}J_{PPt}$ = 3086.3 Hz).

Complex 5. A pressure NMR tube containing a solution of **2** (50 mg, 0.052 mmol) in CD_2Cl_2 (0.3 mL) was loaded with dihydrogen (3 bar) and heated at 80 °C during 10h. Then the volatiles were removed under vacuum. The product was extracted with DCM (0.4 mL). The addition of pentane (0.4 mL) to the DCM solution gives the expected compound **5** as a clear yellow solid with a yield of 80%. HRMS (ESI): exact mass (monoisotopic) calcd for $[C_{44}H_{43}P_2Pt]^+$: $[M - (Al tBu_2{+}H_2)]^+$, 827.2467; found, 827.2480. ^{1}H NMR (500 MHz, 20 °C, C_6D_6, δ): − 8.64 (ddd, 1H, $^{2}J_{HH}$ = 20.2 Hz, $^{2}J_{H\text{-}PPh3}$ = 20.4 Hz, $^{2}J_{H\text{-}PMes2}$ = 6.6 Hz, $^{1}J_{HPt}$ = 1023.3 Hz, HPt), − 3.54 (ddd, 1H, $^{2}J_{HH}$ = 20.2 Hz, $^{2}J_{H\text{-}PPh3}$ = 11.2 Hz, $^{2}J_{H\text{-}PMes2}$ = 6.3 Hz, $^{1}J_{HPt}$ = 691.3 Hz, Al···HPt), 1.03 (s, 18H, *t*Bu), 2.07 (s, 6H, $CH_{3p\text{-}Mes}$), 2.76 (s, 12H, $CH_{3o\text{-}Mes}$), 6.75 (d, 4H, $^{4}J_{HP}$ = 2.9 Hz, $H_{m\text{-}Mes}$), 6.96−7.07 (m, 10H, $H_{p\text{-}Ar}$ and $H_{o\text{-}Ar'}$ and $H_{p\text{-}Ar'}$), 7.18 (m, 2H, $H_{m\text{-}Ar}$), 7.36 (d, 1H, $^{3}J_{HP}$ = 42.3 Hz, HCCP), 7.56 (m, 2H, $H_{o\text{-}Ar}$), 7.71 (dm, 6H, $H_{m\text{-}Ar'}$). ^{13}C{^{1}H} NMR (126 MHz, 20 °C, C_6D_6, δ): 18.0 (s br., 2C, Al(C(CH$_3$)$_3$)$_2$), 20.8 (s, 2C, $CH_{3p\text{-}Mes}$), 26.4 (d, 4C, $^{3}J_{CP}$ = 6.9 Hz, $CH_{3o\text{-}Mes}$), 32.9 (s, 6C, *t*Bu), 127.9 (s, 2C, $CH_{o\text{-}Ar}$), 128.4 (s, $CH_{p\text{-}Ar}$), 128.5 (d, 6C, $^{2}J_{CP}$ = 10.5 Hz, $CH_{o\text{-}Ar'}$), 129.1 (s, 2C, $CH_{m\text{-}Ar}$), 129.9 (dd, 2C, $^{1}J_{CP}$ = 41.7 Hz, $^{3}J_{CP}$ = 2.1 Hz, $C_{ipso\text{-}Mes}$), 130.6 (d, 3C, $^{4}J_{CP}$ = 2.1 Hz, $CH_{p\text{-}Ar'}$),

DOI: 10.1021/jacs.6b01320
J. Am. Chem. Soc. 2016, 138, 4917−4926

131.6 (d, 4C, $^3J_{CP}$ = 8.2 Hz, $CH_{m\text{-}Mes}$), 134.6 (dd, 3C, $^1J_{CP}$ = 51.5 Hz, $^3J_{CP}$ = 2.6 Hz, $C_{ipso\text{-}Ar'}$), 134.6 (d, 6C, $^3J_{CP}$ = 12.5 Hz, $CH_{m\text{-}Ar'}$), 139.9 (d, 2C, $^4J_{CP}$ = 2.3 Hz, $C_{p\text{-}Mes}$), 141.5 (d, J_{CP} = 28.8 Hz, $C_{quat.}$), 143.7 (dd, 4C, $^2J_{CP}$ = 8.8 Hz, $^4J_{CP}$ = 2.0 Hz, $^3J_{CPt}$ = 19.0 Hz, $C_{o\text{-}Mes}$), 152.3 (dd br., J_{CP} = 22.2 Hz, J_{CP} = 4.3 Hz, J_{CPt} = 20.3 Hz, $C_{quat.}$), 153.5 (dd, $^2J_{CP}$ = 12.2 Hz, $^4J_{CP}$ = 4.9 Hz, $^3J_{CPt}$ = 42.6 Hz, HCCP). $^{31}P\{^1H\}$ NMR (202 MHz, 20 °C, C_6D_6, δ): − 17.3 (d, $^2J_{PP}$ = 363.8 Hz, $^1J_{PPt}$ = 2717.4 Hz), 28.4 (d, $^2J_{PP}$ = 363.8 Hz, $^1J_{PPt}$ = 2662.3 Hz).

Complex 7. A NMR tube containing a solution of **2** (20 mg, 0.021 mmol) in CD_2Cl_2 (0.4 mL) was reacted with benzamide (2.5 mg, 0.021 mmol) during 1h at r.t. The solution was concentrated and pentane (0.4 mL) was added. The solution was placed at −20 °C for 10h and the expected product precipitated. The product was obtained as clear yellow crystals by slow diffusion of pentane (0.4 mL) into a concentrated solution of **7** in CD_2Cl_2 at −20 °C in 82% Yield. ^1H NMR (500 MHz, 25 °C, CD_2Cl_2, δ): − 16.44 (dd, 1H, $^2J_{HP}$ = 11.8 Hz, $^2J_{HP}$ = 17.0 Hz, $^1J_{HPt}$ = 965.8 Hz), 0.63 (s br., 18H, *t*Bu), 2.19 (s, 6H, $CH_{3p\text{-}Mes}$), 2.62 (s br., 12H, $CH_{3o\text{-}Mes}$), 5.78 (s br,. 1H, NH), 6.61 (m, 2H, $H_{o\text{-}Ar''}$), 6.73 (s br., 4H, $H_{m\text{-}Mes}$), 7.12 (m, 2H, $H_{m\text{-}Ar''}$), 7.22 (m, 1H, $H_{p\text{-}Ar}$), 7.26 (m, 1H, $H_{p\text{-}Ar''}$), 7.31 (m, 2H, H_{Ar}), 7.38 (m, 2H, H_{Ar}), 7.43 (m, 6H, $H_{o\text{-}Ar'}$), 7.49 (m, 4H, $H_{p\text{-}Ar'}$ and HCCP), 7.59 (m, 6H, $H_{m\text{-}Ar'}$). $^{13}C\{^1H\}$ NMR (126 MHz, 25 °C, CD_2Cl_2, δ): 17.8 (s br., 2C, $Al(\underline{C}(CH_3)_3)_2$), 20.9 (s, 4C, $CH_{3o\text{-}Mes}$), 27.3 (s br., 2C, $CH_{3p\text{-}Mes}$), 33.0 (s, 6C, *t*Bu), 127.1 (s, 2C, $CH_{o\text{-}Ar''}$), 127.5 (s, 1C, $CH_{p\text{-}Ar}$), 128.0 (s, 4C, $CH_{m\text{-}Ar''}$ and CH_{Ar}), 128.9 (s, 2C, CH_{Ar}), 129.1 (d, 6C, J_{CP} = 10.9 Hz, $CH_{o\text{-}Ar'}$), 130.2 (s, 1C, $CH_{p\text{-}Ar''}$), 131.3 (d, 3C, J_{CP} = 1.9 Hz, $CH_{p\text{-}Ar'}$), 131.4 (d br., 4C, J_{CP} = 7.5 Hz, $CH_{m\text{-}Mes}$), 131.9 (dd, 3C, J_{CP} = 2.9 Hz, J_{CP} = 51.7 Hz, $C_{ipso\text{-}Ar'}$), 133.3 (d, 1C, J_{CP} = 39.8 Hz, C_{quat}), 134.8 (d, 6C, J_{CP} = 12.0 Hz, $CH_{m\text{-}Ar'}$), 138.2 (s, 1C, $C_{ipso\text{-}Ar''}$), 140.0 (d, 2C, J_{CP} = 2.0 Hz, $C_{p\text{-}Mes}$), 143.9 (d, 4C, J_{CP} = 29.2 Hz, $C_{o\text{-}Mes}$), 156.7 (dd, 1C, J_{CP} = 4.4 Hz, J_{CP} = 9.7 Hz, HCCP), 174.9 (s br, 1C, O<u>C</u>N). $^{31}P\{^1H\}$ NMR (202 MHz, 25 °C, CD_2Cl_2, δ): 12.5 (d, $^2J_{PP}$ = 385 Hz, $^1J_{PPt}$ = 2998.9 Hz), 26.9 (d, $^2J_{PP}$ = 385 Hz, $^1J_{PPt}$ = 2889.5 Hz).

■ ASSOCIATED CONTENT

Supporting Information

The Supporting Information is available free of charge on the ACS Publications website at DOI: 10.1021/jacs.6b01320.

Analytical data, computational and crystallographic details (PDF)
X-ray diffraction data (CIF)
Optimized structures (XYZ)

■ AUTHOR INFORMATION

Corresponding Authors

*bouhadir@chimie.ups-tlse.fr
*j.c.slootweg@vu.nl
*uhlw@uni-muenster.de
*dbouriss@chimie.ups-tlse.fr

Author Contributions

$^{\nabla}$M.D., R.D., and E.N. contributed equally to this work.

Notes

The authors declare no competing financial interest.

■ ACKNOWLEDGMENTS

This work was supported financially by the Centre National de la Recherche Scientifique (CNRS), the Université Paul Sabatier (UPS), French MESR (Ph.D. grant to R.D.), the Deutsche Forschungsgemeinschaft, the COST Action CM1205 CARISMA (Catalytic Routines for Small Molecule Activation), the European Union (Marie Curie ITN SusPhos, Grant Agreement No. 317404), the Council for Chemical Sciences of The Netherlands Organization for Scientific Research (NWO/CW) by a VIDI grant (J.C.S.), and the PHC Van Gogh program (PROJECT N8 31616SK). We are grateful to Amos Rosenthal for his assistance with the XRD analysis of the CS_2 adduct **4**.

■ REFERENCES

(1) Amgoune, A.; Bourissou, D. *Chem. Commun.* **2011**, *47*, 859.
(2) (a) Kuzu, I.; Krummenacher, I.; Meyer, J.; Armbruster, F.; Breher, F. *Dalton Trans.* **2008**, 5836. (b) Fontaine, F. G.; Boudreau, J.; Thibault, M. H. *Eur. J. Inorg. Chem.* **2008**, *2008*, 5439. (c) Bouhadir, G.; Amgoune, A.; Bourissou, D. *Adv. Organomet. Chem.* **2010**, *58*, 1. (d) Kameo, H.; Nakazawa, H. *Chem. - Asian J.* **2013**, *8*, 1720. (e) Amgoune, A.; Bouhadir, G.; Bourissou, D. *Top. Curr. Chem.* **2012**, *334*, 281.
(3) (a) Parkin, G. *Organometallics* **2006**, *25*, 4744. (b) Hill, A. F. *Organometallics* **2006**, *25*, 4741. (c) Sircoglou, M.; Bontemps, S.; Mercy, M.; Saffon, N.; Takahashi, M.; Bouhadir, G.; Maron, L.; Bourissou, D. *Angew. Chem., Int. Ed.* **2007**, *46*, 8583.
(4) Complexes of ambiphilic ligands open different possibilities of catalytic relevance. Besides TM/LA cooperativity, the Lewis acid moiety can act as an anchor toward incoming substrates, it can abstract a coligand at the metal and generate thereby zwitterionic complexes, and it can behave as a weak and adaptative ligand able to stabilize complexes of different electronic and geometric environments. See: (a) Bouhadir, G.; Bourissou, D. *Chem. Soc. Rev.* **2016**, *45*, 1065. (b) Bouhadir, G.; Bourissou, D. In *Ligand Design in Transition Metal Chemistry*; Lundgren, R.; M.. Stradiotto, Eds.; Wiley: in press.
(5) (a) Grützmacher, H. *Angew. Chem., Int. Ed.* **2008**, *47*, 1814. (b) Gunanathan, C.; Milstein, D. *Acc. Chem. Res.* **2011**, *44*, 588. (c) Devillard, M.; Bouhadir, G.; Bourissou, D. *Angew. Chem., Int. Ed.* **2015**, *54*, 730.
(6) (a) For an overview of hydrogen storage with metal borane complexes, see: Owen, G. R. *Chem. Soc. Rev.* **2012**, *41*, 3535. (b) Harman, W. H.; Peters, J. C. *J. Am. Chem. Soc.* **2012**, *134*, 5080. (c) Zeng, G.; Sakaki, S. *Inorg. Chem.* **2013**, *52*, 2844. (d) Harman, W. H.; Lin, T. P.; Peters, J. C. *Angew. Chem., Int. Ed.* **2014**, *53*, 1081. (e) Barnett, B. R.; Moore, C. E.; Rheingold, A. L.; Figueroa, J. S. *J. Am. Chem. Soc.* **2014**, *136*, 10262. (f) Cowie, B. E.; Emslie, D. J. H. *Chem. - Eur. J.* **2014**, *20*, 16899. (g) Li, Y.; Hou, C.; Jiang, J.; Zhang, Z.; Zhao, C.; Page, A. J. *ACS Catal.* **2016**, *6*, 1655.
(7) For catalytic olefin hydrogenation involving heavier group 13 elements as σ-acceptors, see: Cammarota, R. C.; Lu, C. C. *J. Am. Chem. Soc.* **2015**, *137*, 12486.
(8) (a) Devillard, M.; Nicolas, E.; Appelt, C.; Backs, J.; Mallet-Ladeira, S.; Bouhadir, G.; Slootweg, J. C.; Uhl, W.; Bourissou, D. *Chem. Commun.* **2014**, *50*, 14805. (b) Devillard, M.; Nicolas, E.; Ehlers, A. W.; Backs, J.; Mallet-Ladeira, S.; Bouhadir, G.; Slootweg, J. C.; Uhl, W.; Bourissou, D. *Chem. - Eur. J.* **2015**, *21*, 74.
(9) (a) Bouhadir, G.; Bourissou, D. In *The Chemical Bond - 100 years old and getting stronger*; Structure and Bonding; Mingos, M., Ed.; Springer, in press. (b) Layh, M.; Uhl, W.; Bouhadir, G.; Bourissou, D. In *Patai's Chemistry of Functional Groups: Organoaluminum Compounds*; Rappoport, Z.; Liebman, J. F.; Marek, I., Eds.; John Wiley & Sons, in press.
(10) Bessel, C. A.; Aggarwal, P.; Marschilok, A. C.; Takeuchi, K. J. *Chem. Rev.* **2001**, *101*, 1031.
(11) (a) Appelt, C.; Westenberg, H.; Bertini, F.; Ehlers, A. W.; Slootweg, J. C.; Lammertsma, K.; Uhl, W. *Angew. Chem., Int. Ed.* **2011**, *50*, 3925. (b) Roters, S.; Appelt, C.; Westenberg, H.; Hepp, A.; Slootweg, J. C.; Lammertsma, K.; Uhl, W. *Dalton Trans.* **2012**, *41*, 9033. (c) Bertini, F.; Hoffmann, F.; Appelt, C.; Uhl, W.; Ehlers, A. W.; Slootweg, J. C.; Lammertsma, K. *Organometallics* **2013**, *32*, 6764. (d) Uhl, W.; Appelt, C. *Organometallics* **2013**, *32*, 5008. (e) Uhl, W.; Appelt, C.; Backs, J.; Westenberg, H.; Wollschläger, A.; Tannert, J. *Organometallics* **2014**, *33*, 1212.
(12) Cordero, B.; Gomez, V.; Platero-Prats, A. E.; Reves, M.; Echeverria, J.; Cremades, E.; Barragan, F.; Alvarez, S. *Dalton Trans.* **2008**, 2832.
(13) For cage complexes featuring M→Al interactions, see: (a) Rudd, P. A.; Liu, S.; Gagliardi, L.; Young, V. G.; Lu, C. C. *J. Am. Chem. Soc.*

DOI: 10.1021/jacs.6b01320
J. Am. Chem. Soc. 2016, 138, 4917−4926

2011, *133*, 20724. (b) Sircoglou, M.; Saffon, K.; Miqueu, K.; Bouhadir, G.; Bourissou, D. *Organometallics* **2013**, *32*, 6780.
(14) (a) Braunschweig, H.; Gruss, K.; Radacki, K. *Angew. Chem., Int. Ed.* **2007**, *46*, 7782. (b) Bauer, J.; Braunschweig, H.; Brenner, P.; Kraft, K.; Radacki, K.; Schwab, K. *Chem. - Eur. J.* **2010**, *16*, 11985. (c) Bauer, J.; Braunschweig, H.; Damme, A.; German, s. l.; Radacki, K. *Chem. Commun.* **2011**, *47*, 12783. (d) Bauer, J.; Bertermann, R.; Braunschweig, H.; Gruss, K.; Hupp, F.; Kramer, T. *Inorg. Chem.* **2012**, *51*, 5617.
(15) (a) Chai, J.-D.; Head-Gordon, M. *Phys. Chem. Chem. Phys.* **2008**, *10*, 6615. (b) Chai, J.-D.; Head-Gordon, M. *J. Chem. Phys.* **2008**, *128*, 084106.
(16) *Gaussian 09*, Revision D.01; Frisch, M. J.; Trucks, G. W.; Schlegel, H. B.; Scuseria, G. E.; Robb, M. A.; Cheeseman, J. R.; Scalmani, G.; Barone, V.; Mennucci, B.; Petersson, G. A.; Nakatsuji, H.; Caricato, M.; Li, X.; Hratchian, H. P.; Izmaylov, A. F.; Bloino, J.; Zheng, G.; Sonnenberg, J. L.; Hada, M.; Ehara, M.; Toyota, K.; Fukuda, R.; Hasegawa, J.; Ishida, M.; Nakajima, T.; Honda, Y.; Kitao, O.; Nakai, H.; Vreven, T.; Montgomery, Jr., J. A.; Peralta, J. E.; Ogliaro, F.; Bearpark, M.; Heyd, J. J.; Brothers, E.; Kudin, K. N.; Staroverov, V. N.; Kobayashi, R.; Normand, J.; Raghavachari, K.; Rendell, A.; Burant, J. C.; Iyengar, S. S.; Tomasi, J.; Cossi, M.; Rega, N.; Millam, N. J.; Klene, M.; Knox, J. E.; Cross, J. B.; Bakken, V.; Adamo, C.; Jaramillo, J.; Gomperts, R.; Stratmann, R. E.; Yazyev, O.; Austin, A. J.; Cammi, R.; Pomelli, C.; Ochterski, J. W.; Martin, R. L.; Morokuma, K.; Zakrzewski, V. G.; Voth, G. A.; Salvador, P.; Dannenberg, J. J.; Dapprich, S.; Daniels, A. D.; Farkas, Ö.; Foresman, J. B.; Ortiz, J. V.; Cioslowski, J.; Fox, D. J., Gaussian, Inc.: Wallingford, CT, 2009.
(17) For reviews on CO_2 complexes, see: (a) Pandey, K. K. *Coord. Chem. Rev.* **1995**, *140*, 37. (b) Gibson, D. H. *Chem. Rev.* **1996**, *96*, 2063. (c) Gibson, D. H. *Coord. Chem. Rev.* **1999**, *185−186*, 335.
(18) Two independent molecules with similar features were observed in the crystalline unit. See Chart S2 (SI) for the metric data of the second molecule.
(19) For selected examples, see: (a) Carr, N.; Mole, L.; Orpen, A. G.; Spencer, J. L. *J. Chem. Soc., Dalton Trans.* **1992**, 2653. (b) Spencer, J. L.; Mhinzi, G. S. *J. Chem. Soc., Dalton Trans.* **1995**, 3819. (c) Baratta, W.; Stoccoro, S.; Doppiu, A.; Herdtweck, E.; Zucca, A.; Rigo, P. *Angew. Chem., Int. Ed.* **2003**, *42*, 105. (d) Ingleson, M. J.; Mahon, M. F.; Weller, A. S. *Chem. Commun.* **2004**, 2398. (e) Crosby, S. H.; Clarkson, G. J.; Rourke, J. P. *J. Am. Chem. Soc.* **2009**, *131*, 14142. (f) Rivada-Wheelaghan, O.; Donnadieu, B.; Maya, C.; Conejero, S. *Chem. - Eur. J.* **2010**, *16*, 10323. (g) Omae, I. *J. Organomet. Chem.* **2011**, *696*, 1128. (h) Campos, J.; Peloso, R.; Carmona, E. *Angew. Chem., Int. Ed.* **2012**, *51*, 8255. (i) Campos, J.; Ortega-Moreno, L.; Conejero, S.; Peloso, R.; Lopez-Serrano, J.; Maya, C.; Carmona, E. *Chem. - Eur. J.* **2015**, *21*, 8883.
(20) For a review on three-coordinate T-shape Pt complexes, see: Ortuño, M. A.; Conejero, S.; Lledós, A. *Beilstein J. Org. Chem.* **2013**, *9*, 1352.
(21) At room temperature, the four *ortho*-Me groups of the Mes fragments are magnetically equivalent (δ ^{1}H 2.32 and ^{13}C 23.9 ppm), but at − 90 °C, these signals are split into four resonances of equal intensity. No H−Pt coupling is observed, but the coordination of one CH_3 group to Pt is supported by the significant high-field shift of a ^{13}C NMR signal (δ 15.8 ppm).
(22) According to a Cambridge database search, only two complexes (Rh and Ru) with η^1-CO_2 have been structurally characterized, see: (a) Calabrese, J. C.; Herskovitz, T.; Kinney, J. B. *J. Am. Chem. Soc.* **1983**, *105*, 5914. (b) Tanaka, H.; Nagao, H.; Peng, S. M.; Tanaka, K. *Organometallics* **1992**, *11*, 1450.
(23) For η^1-CO_2 complexes characterized by NMR in solution, see: (a) Aresta, M.; Nobile, C. F. *Inorg. Chim. Acta* **1977**, *24*, L49. (b) Herskovitz, T. *J. Am. Chem. Soc.* **1977**, *99*, 2391.
(24) (a) Aresta, M.; Nobile, C. F.; Albano, V. G.; Forni, E.; Manassero, M. *J. Chem. Soc., Chem. Commun.* **1975**, *0*, 636. (b) Aresta, M.; Nobile, C. F. *J. Chem. Soc., Dalton Trans.* **1977**, 708. (c) Anderson, J. S.; Iluc, V. M.; Hillhouse, G. L. *Inorg. Chem.* **2010**, *49*, 10203. (d) Beck, R.; Shoshani, M.; Krasinkiewicz, J.; Hatnean, J. A.; Johnson, S. A. *Dalton Trans.* **2013**, *42*, 1461. (e) A shift from η^2- to η^1-CO_2 coordination was observed upon reaction of a (PPP) Ni complex with $B(C_6F_5)_3$: Kim, Y. E.; Kim, J.; Lee, Y. *Chem. Commun.* **2014**, *50*, 11458.
(25) Sakamoto, M.; Shimizu, I.; Yamamoto, A. *Organometallics* **1994**, *13*, 407.
(26) (a) Butler, I. S.; Fenster, A. E. *J. Organomet. Chem.* **1974**, *66*, 161. (b) Werner, H. *Coord. Chem. Rev.* **1982**, *43*, 165. (c) Farrar, D. H.; Gukathasan, R. R.; Morris, S. A. *Inorg. Chem.* **1984**, *23*, 3258. (d) Haack, P.; Limberg, C.; Tietz, T.; Metzinger, R. *Chem. Commun.* **2011**, *47*, 6374. (e) Bheemaraju, A.; Beattie, J. W.; Lord, R. L.; Martin, P. D.; Groysman, S. *Chem. Commun.* **2012**, *48*, 9595.
(27) According to a Cambridge database search, the lengths of the bonds between the divalent S and tetravalent Al center range from 2.15 to 2.51 Å.
(28) Only three Pt CS_2 complexes have been structurally characterized, and two of them are dinuclear species: (a) Mason, R.; Rae, A. I. M. *J. Chem. Soc. A* **1970**, 1767. (b) Farrar, D. H.; Lunniss, J. A. *Acta Crystallogr., Sect. C: Cryst. Struct. Commun.* **1985**, *41*, 1444.
(29) (a) Hope, E. G.; Levason, W. *Coord. Chem. Rev.* **1993**, *122*, 109. (b) Lin, T. P.; Gabbaï, F. P. *J. Am. Chem. Soc.* **2012**, *134*, 12230.
(30) According to a Cambridge database search, the average Pt−H distance in Pt hydride complexes is 1.604 Å but a number of complexes display Pt−H distances close to 1.4 Å. In particular, a similarly short Pt−H distance (1.466 Å) was reported for a related complex with a N−C(=O) fragment in the *trans* position to the hydride, see: Wanjek, H.; Steimann, M.; Beck, W. *Chem. Ber.* **1988**, *121*, 1417.
(31) For a rare example involving F_3CCONH_2 and *in situ* generated Pt(0) precursors, see: Schaad, D. R.; Landis, C. R. *Organometallics* **1992**, *11*, 2024.
(32) Bauer, J.; Braunschweig, H.; Dewhurst, R. D. *Chem. Rev.* **2012**, *112*, 4329.

DOI: 10.1021/jacs.6b01320
J. Am. Chem. Soc. 2016, 138, 4917−4926